Interconverting Receptor States at 4 °C for the Neutrophil N-Formyl Peptide Receptor†

Julie F. Hoffman,‡ Michael L. Keil,§ Todd A. Riccobene,‡ Geneva M. Omann,*,§ and Jennifer J. Linderman‡

Department of Chemical Engineering, University of Michigan, Ann Arbor, Michigan, and Departments of Biological Chemistry and Surgery, University of Michigan Medical School and Veteran's Administration Medical Center, Ann Arbor, Michigan

Received May 7, 1996; Revised Manuscript Received July 23, 1996⊗

ABSTRACT: With the aid of high time resolution kinetic data extracted from a flow cytometer, we determined that there are two N-formyl peptide receptor states for human neutrophils at 4 °C: a low affinity and a high affinity state. Competitive binding of FMLP, FNLP, and t-BOC with FNLPNTL-FL revealed different kinetic rate constants for two distinct reactions that control the lifetime of the low affinity ligand−receptor complex. For these ligands, the rate constant for dissociation of ligand from the low affinity receptor state (the first reaction) ranges in order of magnitude from 10^{-2} to 1 s^{-1}, and the conversion rate constant from the low affinity receptor state to the high affinity receptor state (the second reaction) ranges from 10^{-4} to 10^{-2} s^{-1}. The antagonist t-BOC differed most significantly from the three agonists by having an association rate constant for the low affinity receptor on the order of 10^5 M^{-1} s^{-1}; the value for all three agonists was on the order of 10^7 M^{-1} s^{-1}. Characterization of the receptor conversion at 4 °C revealed that it is irreversible (or very slow) and independent of G_i protein and that neither receptor state is a form of receptor precoupled to G_i protein. The affinity conversion and the dissociation characteristics of each receptor state determine the duration of the signaling complex and may contribute to differences in ligand efficacy.

Understanding ligand−receptor dynamics is an essential step to understanding the activation of cells by external ligands. Activation of human neutrophils by N-formyl peptides via the N-formyl peptide receptor has been extensively studied (Omann et al., 1987; Baggiolini et al., 1993; Lad et al., 1992; Downey, 1994). Of greatest interest is understanding binding characteristics at physiological temperatures, and numerous studies of ligand binding at 37 °C have been performed (Jesaitis et al., 1983, 1988a,b, 1989; Klotz et al., 1994a,b; Koo et al., 1982; Korchak et al., 1984; Low et al., 1981; Painter et al., 1987; Posner et al., 1994; Sklar et al, 1987; Hoffman et al., 1996). These studies indicate that there are two interconverting affinity states of the N-formyl peptide receptor, a low affinity signaling form and a high affinity, nonsignaling form. At physiological temperatures, receptor processing events such as receptor upregulation and internalization complicate the interpretation of binding data. Complex binding models have been formulated to take all these processes into account (Sklar, 1987; Hoffman et al., 1996). However, to gain confidence in the values obtained for binding rate constants at 37 °C, reduced models are helpful. One strategy for reducing the variables in the model is to reduce the temperature so receptor upregulation and internalization do not occur.

While the existence of two receptor states for the N-formyl peptide receptor at 37 °C has been well documented (Jesaitis et al., 1983, 1988a,b, 1989; Klotz et al., 1994; Klotz & Jesaitis, 1994; Koo et al., 1982; Korchak et al., 1984; Low et al., 1981; Painter et al., 1987; Posner et al., 1994; Sklar et al., 1987; Sklar, 1987; Hoffman et al., 1996), there are conflicting reports about the presence of two affinity states at 4 °C. The following one-site model has been extensively used to describe both dynamic and equilibrium states of N-formyl peptide binding to the N-formyl peptide receptor at 4 °C (Goldman et al., 1986; Korchack et al., 1984; Mueller et al., 1991; Sklar et al., 1985a; Tennenberg et al., 1988):

$$L + R_s \underset{k_r}{\overset{k_f}{\rightleftharpoons}} LR_s \qquad \text{(Model I)}$$

where R_s is a homogeneous, monovalent population of surface receptors (number/cell), L is the free ligand concentration (M), and LR_s is the number of ligand−receptor complexes (number/cell) which form with an association rate constant of k_f (M^{-1} s^{-1}) and are lost with a dissociation rate constant of k_r (s^{-1}).

A few studies, however, report that a two affinity state model provides a significantly better fit of N-formyl peptide binding data at 4 °C over the one-site model shown above. One investigation utilized human neutrophil membrane preparations (Koo et al., 1982), and two others used intact rabbit neutrophils (Vitkauskas et al., 1980; Zigmond & Tranquillo, 1986). Since it is possible that the process of extracting membranes may change the affinity of a receptor for its ligand, results from binding experiments with membrane preparations may not reflect the affinity of receptors in their native state and should be interpreted with caution.

† This work was supported by National Science Foundation Grant No. BES-9410403, the Office of Research and Development, Medical Research Service, Department of Veteran's Affairs, University of Michigan Department of Surgery RAC Grant, and NIH Training Grant No. GM08353 (Cellular Biotechnology Training Program, University of Michigan).

* To whom correspondence should be directed. Research Service (151), Veteran's Administration Medical Center, 2215 Fuller Road, Ann Arbor, MI 48105. Telephone: (313) 769-7100, ext. 5238. Fax: (313) 761-7693. E-mail: gmomann@umich.edu.

‡ Department of Chemical Engineering, University of Michigan.

§ Departments of Biological Chemistry and Surgery, University of Michigan Medical School and Veteran's Administration Medical Center.

⊗ Abstract published in *Advance ACS Abstracts,* September 15, 1996.

S0006-2960(96)01088-4 CCC: $12.00

The studies by Zigmond and Tranquillo (1986) and Vitkauskas et al. (1980) were performed in whole cells with tritiated N-formyl-Nle-Leu-Phe (FNLP).[1] In both studies, ligand dissociation data revealed two dissociating components. In addition, the study by Zigmond and Tranquillo (1986) determined that the observed rate of accumulation of ligand in the high affinity compartment was proportional to the ligand bound to the low affinity compartment. This latter observation suggests that the high affinity component is derived from the conversion of the low affinity compartment.

We report here that there are two affinity states of the receptor for bound N-formyl peptides N-formylnorleucylleucylphenylalanylnorleucyltyrosyllysine fluorescein (FNLPNTL-FL), F-Met-Leu-Phe (FMLP), FNLP, and the N-formyl peptide receptor antagonist t-Boc-Phe-D-Leu-Phe-D-Leu-Phe-OH (t-BOC). We show not only that the rate constants for ligand dissociation are ligand-specific but also that the rate constant for conversion from a low to a high affinity receptor state is ligand-dependent. Characterization of the conversion at 4 °C revealed that it is irreversible (or extremely slow) and independent of G_i protein.

MATERIALS AND METHODS

Isolation of Neutrophils. Human neutrophils were isolated from citrated blood by the elutriation method of Tolley et al. (1987). Cells were stored at 4 °C in buffer without added Ca^{2+} (HSB) containing 5 mM KCl, 147 mM NaCl, 1.9 mM KH_2PO_4, 0.22 mM Na_2HPO_4, 5.5 mM glucose, 0.3 mM $MgSO_4$, 1 mM $MgCl_2$, and 10 mM HEPES, at pH 7.4. Assays and binding studies were performed in HSB with 1.5 mM $CaCl_2$.

Equilibrium Binding Assay. An equilibrium ligand binding assay, described in Sklar and Finney (1982), was used to determine the number of N-formyl peptide receptors on the plasma membrane surface (R_s). FNLPNTL-FL (Molecular Probes, Eugene, OR) stocks were made in dimethyl sulfoxide (DMSO) and were diluted to <0.1% DMSO in HSB plus 0.1% bovine serum albumin (BSA) vehicle. Cells at 1×10^6/mL were equilibrated with 0.25, 0.50, 0.75, 1.0, and 3 nM FNLPNTL-FL in duplicate on ice for 2 h. A flow cytometer (FACScan, Becton-Dickinson), calibrated with fluorescein isothiocyanate-labeled beads (Quantum 24, Flow Cytometry Standards, Research Triangle Park, NC), was used to quantify fluorescence binding per cell. Neutrophils were gated on the basis of forward and side scatter parameters. Nonspecific binding was determined in the presence of 3×10^{-5} M FMLP (Sigma Chemical Co.). Data for specific binding in fluorescein equivalents were converted to FNLPNTL-FL number per cell using a conversion factor of 1.22 FNLPNTL-FL equivalents/fluorescein equivalent as determined in Fay et al. (1991). The calibration of the standard beads was validated as described by Fay et al. (1991) and found to be accurate within 6% of the nominal fluorescein equivalents given by the manufacturer. Thus the nominal values for fluorescein equivalents per bead provided by the manufacturer were used for converting mean channel number to fluorescein equivalents per cell. Nonlinear regression of FNLPNTL-FL bound/cell versus free ligand using the equilibrium solution of Model I yielded the total number of receptors on the cell surface and the equilibrium dissociation constant (K_d).

Equilibrium Binding Assay for Unlabeled Ligands. An equilibrium binding assay for determining the K_d of an unlabeled ligand was performed and analyzed using a classic competitive binding protocol described in Kenakin (1991). Fractional receptor occupancy of FNLPNTL-FL (at 0.5, 1.0, or 3.0 nM) was measured in the presence of a range of concentrations of nonfluorescent ligand after co-equilibration of binding for 2 h on ice. Data were fit to a single site model (Model I) assuming both ligands bind to the same receptor using

$$\frac{[LR]}{R_{tot}} = \frac{[L]}{\frac{K_{d_l}}{K_{d_a}}([A] + K_{d_a}) + [L]} \quad (1)$$

where [L] is the concentration of FNLPNTL-FL (M), [A] is the concentration of unlabeled ligand (M), $[LR]/R_{tot}$ is the fractional occupancy of FNLPNTL-FL, and K_{d_l} and K_{d_a} are the equilibrium dissociation constants for FNLPNTL-FL and unlabeled ligand, respectively.

Pertussis Toxin (PT) Treatment. A stock of 50 μg/mL PT in 50 mM Tris, 10 mM glycine, 0.5 M NaCl, and 50% glycerol, pH 7.5, was obtained from Sigma Biochemicals. Cells were resuspended with and without PT at 10^8/mL in a sterile, modified Krebs-Ringer buffer with 5.5 mM glucose, 25 mM HEPES, and 6.3 mg/mL cytochrome *c*. Controls and samples with PT (5.0 μg/mL) were incubated at 37 °C with constant rocking for 2 h. Controls consisted of an equivalent amount of PT buffer without PT. Following incubation, cells were then washed in HSB, strained through nylon mesh to remove aggregates, and resuspended in HSB at 10^8/mL. Trypan blue exclusion revealed a viability of >90% following the PT treatment. The efficiency of the PT treatment was monitored with a right angle light scatter assay as described in Sklar et al. (1985c) and with an oxidant assay as described in Hyslop and Sklar (1984). At this treatment level, no right angle light scatter or oxidant response to 100 nM FMLP stimulation was observed.

Kinetic Binding Data Collection. Four kinetic binding protocols (A−D), based on methods described in Sklar et al. (1985a), were used to collect data for determining association and dissociation rate constants for FNLPNTL-FL and unlabeled ligands. Binding data were collected on a flow cytometer, and the assay temperature of 4 °C (±0.4 °C) was maintained by submerging sample tubes in ice contained in insulated beakers. Protocols A and B were used to determine the rate constants associated with FNLPNTL-FL binding in the absence of any other ligand, while protocols C and D were used to determine rate constants associated with the binding of an unlabeled ligand in competition with FNLPNTL-FL.

Protocol A: Association of FNLPNTL-FL. Cells at 10^6/mL in HSB plus Ca^{2+} were placed on the flow cytometer, and the flow of cells was initiated to start the internal clock and obtain baseline values for forward scatter, side scatter, and cell autofluorescence using LYSIS II software (Becton Dickinson). At 10 s, the tube of cells was taken from the instrument, and 0.5−3 nM FNLPNTL-FL was added with vortexing (the exact time of FNLPNTL-FL addition was noted). The tube was immediately placed back onto the

[1] Abbreviations: FNLP, *N*-formylnorleucylleucylphenylalanine; FNLPNTL-FL, *N*-formylnorleucylleucylphenylalanylnorleucyltyrosyllysine fluorescein; FMLP, *N*-formylmethionylleucylphenylalanine; K_d, equilibrium dissociation constant; PT, pertussis toxin; t-BOC, t-Boc-Phe-D-Leu-Phe-D-Leu-Phe-OH.

instrument. Data collection resumed in less than 3 s after the addition of ligand and was continued for a total of 3 min or until data for approximately 85 000 cells were collected.

Protocol B: Dissociation of FNLPNTL-FL. Cells at 10^6/mL in HSB plus Ca^{2+} were preincubated with 0.5−3 nM FNLPNTL-FL for 10 s, approximately 90 s, and approximately 2 h. After prebinding, the sample was placed on the flow cytometer, and the extent of ligand bound for each designated time was determined. The binding of FNLPNTL-FL was interrupted by adding 3×10^{-5} M FMLP, and data were collected for a total of 3 min.

Protocol C: Competitive Association of FNLPNTL-FL and Unlabeled Ligand. Baseline values for the fluorescence of cells at 10^6/mL in HSB plus Ca^{2+} were taken as in protocol A. At 10 s, the tube of cells was taken from the flow cytometer, and an aliquot of premixed FNLPNTL-FL and unlabeled ligand were added with vortexing. The tube was immediately returned to the flow cytometer, and data were collected as in protocol A. Concentrations of unlabeled ligand [FMLP, FNLP (Sigma Chemicals), and t-BOC (Bachem, CA)] were varied to obtain several different extents of inhibition of FNLPNTL-FL binding.

Protocol D: Displacement of Unlabeled Ligand by FNLPNTL-FL. Unlabeled ligand (FMLP, FNLP, and t-BOC) was preincubated with cells at 10^6/mL in HSB plus Ca^{2+} for up to 125 s and for 2 h before placing on the flow cytometer to obtain baseline values for parameters as in protocol A. After 10 s, 0.5−3 nM FNLPNTL-FL was added, and data were collected as described in protocol A.

Kinetic Binding Data Analysis. To analyze kinetic data, we developed a protocol to extract and convert data files from the Becton Dickinson FACScan Pascal data format to an ASCII format. Data were first converted to DOS-readable binary files using OSWEGO software (Oswego, IL), uploaded to a UNIX platform, and then converted to ASCII. Neutrophils were gated with a rectangular mask based on forward and side scatter parameters. Forward scatter, side scatter, and fluorescence data collected during each 200 ms time interval (typically 30−200 cells depending on cell concentration and flow rate) were averaged. Fluorescence values were converted to numbers of bound receptors using the calibration scheme described in the equilibrium binding assay. Nonspecific binding of FNLPNTL-FL was characterized in the presence of 3×10^{-5} M FMLP, yielding a linear function with time. Binding data versus time, corrected for nonspecific binding, were loaded into SimuSolv (Dow Chemical, Midland, MI), a simulation package that simultaneously solves differential equations and estimates unknown parameters by maximizing a least log likelihood function.

A set of two-site binding models (one for FNLPNTL-FL and the other for the unlabeled agonist or antagonist) was utilized to fit binding data at 4 °C:

$$L + R_s \underset{k_r}{\overset{k_f}{\rightleftharpoons}} LR_s \xrightarrow{k_c} LR_n \underset{k_{f_n}}{\overset{k_{r_n}}{\rightleftharpoons}} L + R_n$$

$$A + R_s \underset{k_{r_2}}{\overset{k_{f_2}}{\rightleftharpoons}} AR_s \xrightarrow{k_{c_2}} AR_n \underset{k_{f_{n2}}}{\overset{k_{r_{n2}}}{\rightleftharpoons}} A + R_n \qquad \text{(Model II)}$$

where L and A are the concentrations (M) of FNLPNTL-FL and unlabeled competitor, respectively. R_s, LR_s, k_f, and k_r are as defined in model I; R_s is the low affinity form of the receptor. AR_s is the low affinity competitor−receptor complex (no./cell); LR_n and AR_n are the high affinity receptor complexes of bound FNLPNTL-FL and unlabeled competitor, respectively (no./cell); R_n is the high affinity receptor (no./cell); k_{f_2} (M^{-1} s^{-1}) and k_{r_2} (s^{-1}) are the rate constants for association and dissociation of unlabeled competitor to the low affinity receptor, respectively; k_c and k_{c_2} are rate constants for the irreversible[2] conversion from low to high affinity receptor for FNLPNTL-FL and unlabeled ligand, respectively (s^{-1}); k_{r_n} and $k_{r_{n2}}$ are the high affinity receptor dissociation rate constants for FNLPNTL-FL and unlabeled competitor, respectively (s^{-1}); k_{f_n} and $k_{f_{n2}}$ are the high affinity receptor association rate constants for FNLPNTL-FL and unlabeled competitor, respectively (M^{-1} s^{-1}). Differential equations for this model are detailed in the Appendix.

Estimates for binding rate constants were sensitive to the type of data collected; for example, association data (protocols A and C) gave reliable estimates (based on the standard error for the estimate) for binding to and dissociation from R_s, while dissociation data following 2 h of ligand binding (protocols B and D) gave reliable estimates for dissociation from R_n. Thus to obtain reliable estimates for rate constants of FNLPNTL-FL binding, the following analysis protocol was developed and utilized for each donor: (1) Values for the surface receptor number and an equilibrium dissociation constant (K_d) associated with R_n were determined using the 4 °C equilibrium binding curve described above. (2) The association rate constant, k_f, and initial estimates of k_r, k_c, and k_{r_n} for FNLPNTL-FL were determined from fitting association data that were collected as described in protocol A with eqs A.1−A.3 and A.6−A.8 found in the Appendix. Rate constants k_f, k_r, k_c, and k_{r_n} were varied while k_{f_n} was constrained to the value that satisfied the K_d from 4 °C equilibrium binding ($k_{f_n} = k_{r_n}/K_d$). (Sensitivity analysis showed that varying the total receptor number ± the standard error of the mean did not significantly change the values for k_f and k_r.) (3) The rate constant for dissociation of FNLPNTL-FL from the high affinity receptor, k_{r_n}, was determined with greater accuracy than in step 2 by using data from protocol B in which dissociation was initiated after 2 h of binding. The extent of binding at 2 h (LR_n) was determined by averaging the fluorescence of cells before the addition of 3×10^{-5} M FMLP. Since estimates for k_c from step 2 yielded complete conversion from LR_s to LR_n after two hours of FNLPNTL-FL binding (see supporting data in Results), the model was simplified to a one-state model involving only the dissociation of L from LR_n. Thus, the data from Protocol B after 2 h of binding were fit by allowing only one rate constant, k_{r_n}, to vary while k_{f_n} was constrained to equal k_{r_n}/K_d as previously described. (4) To validate k_r and k_c determined in step 2, the rate constants for dissociation of FNLPNTL-FL from the low affinity receptor, k_r, and the conversion from low to high receptor state, k_c, were determined by fits to data from protocol B in which dissociation was initiated after 10 and approximately 90 s of binding using Model II. Rate constants k_r and k_c were varied while k_f and k_{r_n} were held at values determined in steps 2 and 3.

Rate constants for unlabeled ligands (FMLP, FNLP, and t-BOC) were determined by analyzing data in which the

[2] Data fits with models allowing for this step to be reversible yielded no statistical improvement in the fit. It is possible that there is a very slow conversion back to the low affinity state.

unlabeled ligand was in competition with FNLPNTL-FL (protocols C and D). For each donor, the rate constants for FNLPNTL-FL were determined as described above and were then held constant during model fits of competitive binding data. The analysis protocol for determining rate constants of an unlabeled ligand was similar to that described for FNLPNTL-FL. (1) The K_d for the unlabeled ligand was determined following the equilibrium binding assay for unlabeled ligands described in the methods. (2) Competitive association data was collected following protocol C, and k_{f_2} and k_{r_2} were determined by fitting the data with eqs A.1−A.9 (Appendix), allowing k_{f_2}, k_{r_2}, k_{c_2}, and $k_{r_{n2}}$ to vary. (3) Dissociation rate constants for the unlabeled ligand were determined with greater accuracy than in step 2 by using data from the displacement protocol (protocol D). Data analysis for the displacement of unlabeled ligands FMLP, FNLP, and t-BOC after ≥2 h of binding had to be done iteratively. Simulations with a conversion rate constant k_{c2} on the order of 10^{-4} s^{-1} showed that the conversion from the low to high affinity receptor state was not complete after a 2 h preincubation with unlabeled ligand. Because of this, estimates for dissociation rate constants from both the low and high affinity receptor forms, k_{r_2} and $k_{r_{n2}}$, were possible using these data, but the initial number of each of those complexes was unknown. Estimates for the number of AR_s and AR_n complexes accumulated after 2 h of binding were obtained by simulation using k_{f_2} from competitive association experiments, an initial estimate of k_{r_2} from competitive association experiments, and a value of 1×10^{-4} s^{-1} for k_{c_2}. Displacement data (from a 2 h preincubation with the unlabeled ligand) were then fit with the two-site model where the initial values for AR_s and AR_n were estimated as described. Fit values for k_{r_2} and $k_{r_{n2}}$ were then obtained and used to recalculate the initial number of AR_s and AR_n complexes, and displacement data were again fit to refine the estimates for the rate constants. This iteration was continued until there was less than 1% difference in the calculated and initial values for AR_s and AR_n.

The simulation package SimuSolv was used to fit the data. All data fits were statistically evaluated with residuals and a nested likelihood ratio that follows the chi-squared distribution (Seber & Wild, 1989; Mood et al., 1974) and allows comparison between the models of increasing complexity (e.g., Models I and II).

RESULTS

The Association of FNLPNTL-FL at 4 °C Is Biphasic. The time course of specific binding of 3 nM FNLPNTL-FL at 4 °C to the N-formyl peptide receptor and the fits with the one-site model frequently used and our two-site model are shown in Figure 1, panels A and B, respectively. The one-site model clearly underpredicts the data in the first 30 s and overpredicts the data between 30 and 90 s. Evaluation of the two fits using residuals and the least log likelihood function show that a two-site model more accurately describes the association data. A summary of the rate constants associated with the binding of 3 nM FNLPNTL-FL to the N-formyl peptide at 4 °C is given in Table 1. Rate constants from association data were determined with the two-site model (Model II) and the analysis protocol described in Materials and Methods and represent the mean value for 12 different donors.

To validate that the rate constants reported in Table 1 were not dependent upon the ligand concentration, all protocols (A−D) were performed over a range of FNLPNTL-FL concentrations. Figure 2 shows a representative experiment utilizing protocol A. Analysis of variance showed no concentration dependence of calculated rate constants over the range 0.5−3 nM for any of the rate constants in Model II. Thus the data were collected primarily with 3 nM FNLPNTL-FL.

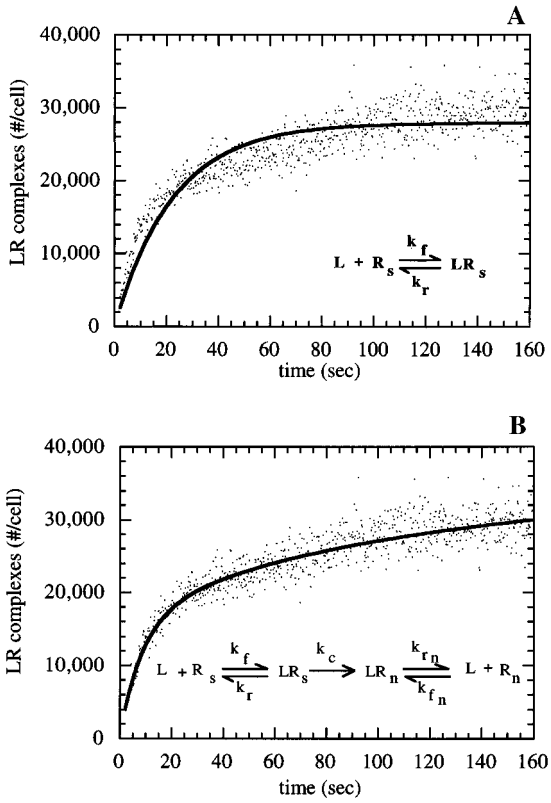

FIGURE 1: Typical fits of one-site (panel A) and two-site (panel B) models for the association of FNLPNTL-FL to human neutrophils at 4 °C. Data were collected using protocol A (adding 3 nM FNLPNTL-FL to cells at 10^6/mL) and were fit as described in Materials and Methods. All fluorescence data were converted to number of bound complexes per cell and are corrected for nonspecific binding. Data are plotted as the total number of LR complexes per cell ($[LR]_{app}$ in the notation of the appendix) versus time in seconds.

Table 1: Rate Constants Obtained Using Two-Site Model Fits to the Binding of 3 nM FNLPNTL-FL at 4 °C

parameter	two-site model[a]
k_f (M^{-1} s^{-1})	$1.1 \pm 0.1 \times 10^{7}$ [b]
k_r (s^{-1})	$6.5 \pm 0.7 \times 10^{-2}$ [b]
	$8.0 \pm 0.3 \times 10^{-2}$ [c]
k_c (s^{-1})	$2.1 \pm 0.3 \times 10^{-2}$ [b]
	$1.3 \pm 0.4 \times 10^{-2}$ [c]
k_{f_n} (M^{-1} s^{-1})	2.0×10^{6} [e]
k_{r_n} (s^{-1})	$7.3 \pm 0.4 \times 10^{-4}$ [c]
	$6.4 \pm 0.5 \times 10^{-4}$ [d]
K_{d,R_s} (M)	6.6×10^{-9} [f]
K_{d,R_n} (M)	$3.5 \pm 2.0 \times 10^{-10}$ [g]

[a] ±the standard error of the mean. [b] Determined from association experiments (protocol A); the number of donors $n = 12$. [c] Determined from dissociation experiments (protocol B, prebound 10 and 60 seconds), $n = 4$. [d] Determined from dissociation experiments (protocol B, prebound 2 h), $n = 4$. [e] For each fit, k_{f_n} was constrained to equal $k_{r_n}/K_{d,R_n}$, where K_{d,R_n} is the equilibrium dissociation constant measured for the high affinity state. [f] K_{d,R_s}, the equilibrium dissociation constant for the low affinity state, was calculated as k_r/k_f, where k_r is the average of the two values reported above. [g] K_{d,R_n} was determined from 4 °C equilibrium binding curves, $n = 12$.

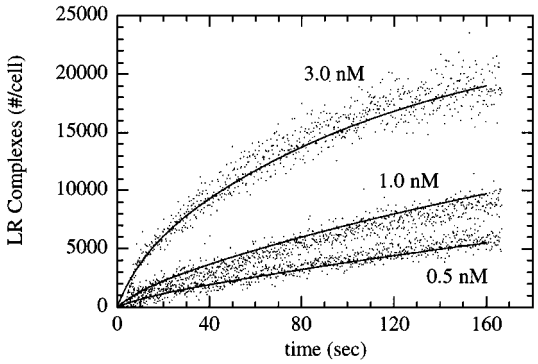

FIGURE 2: Lack of concentration dependence of rate constants determined from association data at 4 °C. Data were collected using protocol A and adding 0.5, 1, or 3 nM FNLPNTL-FL. Data from 3 nM duplicates were fit individually with Model II to obtain rate constants, and average 3 nM rate constants were then computed. These average rate constatns were used to carry out simulations for initial ligand concentrations of 0.5, 1, and 3 nM (solid lines). No systematic bias in the simulations with concentration was noted.

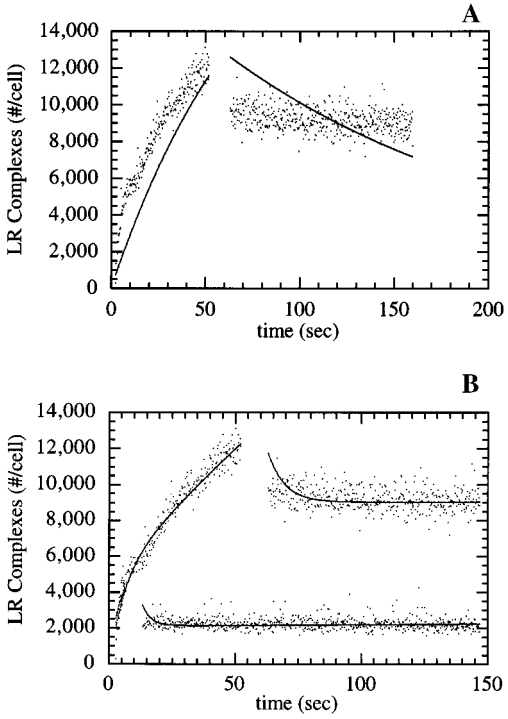

FIGURE 3: Typical fits of one-site (panel A) and two-site (panel B) models for the dissociation of FNLPNTL-FL at 4 °C. Data were collected using protocol B, adding 3 nM FNLPNTL-FL to cells at 10^6/mL at time zero, and interrupting binding with 3×10^{-5} M FMLP after 60 s in panel A and after 10 and 60 s in panel B. Data were corrected for nonspecific binding and fit as described in Materials and Methods.

FNLPNTL-FL Dissociation Data Cannot Be Accounted for with a One-Site Model; the Two-Site Model Affords Estimates for k_r and k_c. Dissociation data revealed two distinct components of dissociation and could not be explained by a model in which only one receptor affinity was allowed. Figure 3A shows a fit of these data with a one-site model and clearly demonstrated its inadequacy in describing FNLPNTL-FL dissociation after 60 s of binding. The two-site model, however, yielded a very good fit to the data (Figure 3B), and mean values for k_r and k_c were determined from fits to dissociation after 10 and approximately 60 s of ligand binding (see Table 1). Mean values for k_r and k_c from dissociation data were not different than those estimated from association data ($p < 0.05$). Results

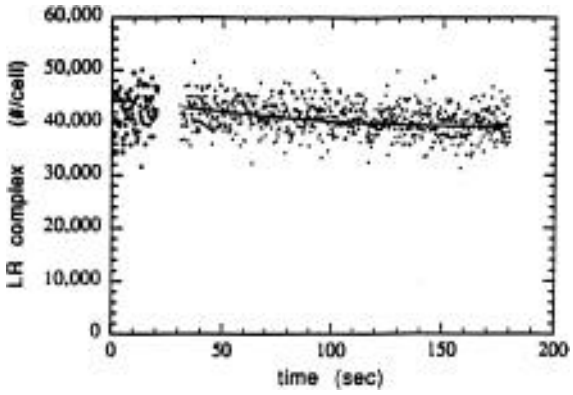

FIGURE 4: Dissociation of FNLPNTL-FL after 2 h of binding at 4 °C. Data were collected using protocol B, adding 3 nM FNLPNTL-FL to cells at 10^6/mL, and interrupting binding with 3×10^{-5} M FMLP 2 h later. In the plot, data collected for the first 20 s represent the quantity of FNLPNTL-FL bound after 2 h. FMLP was added at 25 s. Data indicate the absence of a low affinity state and are best fit with a single exponential yielding an average dissociation rate constant from the high affinity receptor of $(6.4 \pm 0.5) \times 10^{-4}$ s^{-1} ($\pm$ the standard error of the mean, $n = 4$ donors). Data were corrected for nonspecific binding and fit as described in Materials and Methods.

were insensitive to the binding rate constants of FMLP (varied an order of magnitude) due to the excess of FMLP. The ratio of FMLP to FNLPNTL-FL was 10 000:1.

The FNLPNTL-FL-Stimulated Conversion of Receptor from Low to High Affinity Is Irreversible and Is on the Order of 10^{-2} s^{-1}. Figure 4 gives a representative plot of the first 150 s of dissociation of FNLPNTL-FL from the high affinity N-formyl peptide receptor after binding of FNLPNTL-FL at 4 °C for 2 h. Data between 0 and 20 s show the extent of FNLPNTL-FL bound following the 2 h incubation, and data after 30 s show the dissociation of FNLPNTL-FL following the addition of 3×10^{-5} M FMLP. The dissociation data were adequately described with a single exponential, indicating the absence of a low affinity site and the complete conversion of receptors to a high affinity state.

From the two-site model, the effect of the magnitude of the conversion rate constant, k_c, on the depletion of the low affinity state and the formation of the high affinity state can be predicted (Figure 5). For conversion rate constants on the order of 10^{-2} s^{-1}, such as that estimated for the FNLPNTL-FL-stimulated conversion, a significant number of both the low and high affinity receptor complexes are present in the first few minutes of ligand binding, and estimates for k_c obtained from fits to association data and from fits to dissociation data (collected after interrupted binding at 10 and 60 s) are reliable. Using association data, protocol A, we estimated $k_c = 2.1 \times 10^{-2}$ s^{-1} and using dissociation data, protocol B, with binding interrupted at 10 or 60 s, we estimated a value for k_c of 1.3×10^{-2} s^{-1} (Table 1). For conversion rate constants $<10^{-3}$ s^{-1}, the concentration of high affinity ligand−receptor complexes formed within the first 3 min of ligand binding is too low to yield a good estimate for the conversion rate constant from association data, and model fits to data from association and dissociation (initiated in the first couple of minutes of binding) experiments may even yield an estimate for k_c of zero. Examples of this were seen in the fitting of unlabeled ligands and will be discussed presently.

Association and Dissociation Rate Constants for Ligand Binding Were Determined for the Agonists FMLP and FNLP and the Antagonist t-BOC. Rate constants for the association

Table 2: Rate Constants Obtained Using Two-Site Model Fits to Competitive Binding Data Collected Using Protocols C and D[a]

parameter	FMLP	FNLP	t-BOC
k_{f_2} (M^{-1} s^{-1})	$1.2 \pm 0.4 \times 10^7$ ($n = 6$)[b]	$4.0 \pm 1.5 \times 10^7$ ($n = 3$)[b]	$8.3 \pm 0.9 \times 10^5$ ($n = 3$)[b]
k_{r_2} (s^{-1})	$5.5 \pm 1.4 \times 10^{-1}$ ($n = 6$)[b]	2.4 ± 0.6 ($n = 3$)[b]	1.7 ± 0.4 ($n = 3$)[b]
	$6.3 \pm 1.1 \times 10^{-1}$ ($n = 3$)[c]	2.4 ± 0.1 ($n = 2$)[c]	1.4 ± 0.8 ($n = 2$)[c]
k_{c_2} (s^{-1})	$1.1 \pm 0.1 \times 10^{-4}$ ($n = 2$)[d]	$1.0 \pm 0.4 \times 10^{-4}$ ($n = 2$)[d]	$3.9 \pm 2.4 \times 10^{-4}$ ($n = 2$)[d]
$k_{f_{n2}}$ (M^{-1} s^{-1})	470[e]	43[e]	250[e]
$k_{r_{n2}}$ (s^{-1})	$1.6 \pm 0.3 \times 10^{-5}$ ($n = 2$)[d]	$1.3 \pm 0.3 \times 10^{-5}$ ($n = 2$)[d]	$3.8 \pm 0.3 \times 10^{-4}$ ($n = 2$)[d]
K_{d,R_s} (M)	4.9×10^{-8} [f]	6.0×10^{-8} [f]	1.9×10^{-6} [f]
K_{d,R_n} (M)	3.4×10^{-8} [g]	3×10^{-7} [g]	1.5×10^{-6} [g]

[a] Rate constants associated with the binding of FNLPNTL-FL were determined for each donor and were held constant during fits to competitive binding data. Number of donors (n) is indicated. For each donor, assay was performed in duplicate. Data are given as ± the standard error of the mean. [b] Determined from competitive association experiments (protocol C). [c] Determined from displacement experiments, approximately 90 s preequilibration (protocol D). [d] Determined from displacement experiments, approximately 2 h preequilibration (protocol D). [e] During fitting, $k_{f_{n2}}$ was constrained to equal $k_{r_{n2}}/K_{d,R_n}$ where K_{d,R_n} is the equilibrium dissociation constant measured for the high affinity state. The value of $k_{f_{n2}}$ reported in the table is calculated from the value of $k_{r_{n2}}$ and this K_{d,R_n}. [f] K_{d,R_s} was calculated from k_{r_2}/k_{f_2}. [g] K_{d,R_n} was measured from competitive equilibrium binding data as described in Materials and Methods.

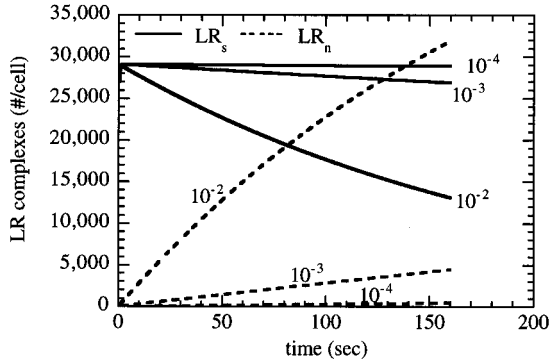

FIGURE 5: Effect of the conversion rate constant, k_c, on the formation of LR_n in the first 160 s of binding at 4 °C. Simulations were run using eqs A.1−A.3 and A.6−A.8 of the two-site model and holding all parameters constant at the values listed in Table 1 except that of k_c. Values for k_c ranged from 10^{-4} to 10^{-2} s^{-1} as indicated in the figure. Solid curves represent the number of low affinity complexes (LR_s) formed over time while the dotted lines represent the number of high affinity complexes (LR_n) formed over time. Simulations run with $k_c = 10^{-2}$ s^{-1} are representative of the conversion stimulated by FNLPNTL-FL while those run for $k_c = 10^{-4}$ s^{-1} are representative of the conversion stimulated by FMLP, FNLP, and t-BOC.

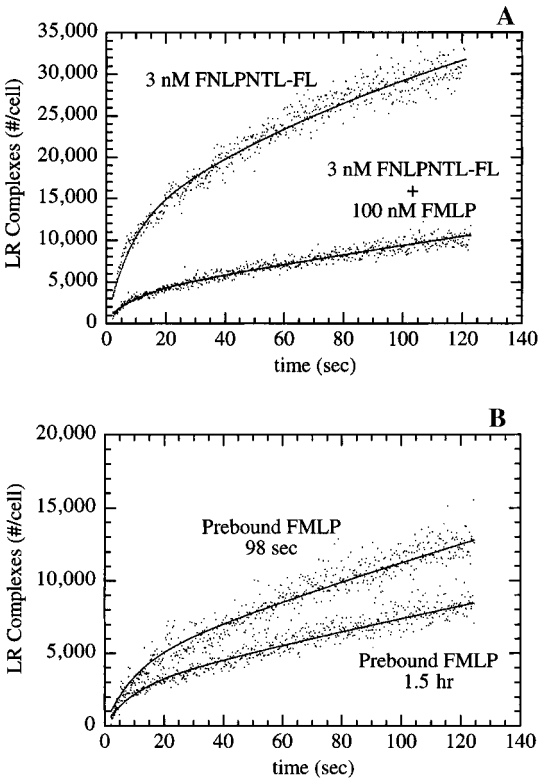

FIGURE 6: (A) Typical fits to FNLPNTL-FL association data and competitive association data. Data were collected using protocol A with the addition of 3 nM FNLPNTL-FL to cells at 10^6/mL at time zero (●) or protocol C with the addition of 3 nM FNLPNTL-FL and 100 nM FMLP simultaneously to cells at 10^6/mL at time zero (▲). Data were corrected for nonspecific binding and fit as described in Materials and Methods. (B) Typical fits to the displacement of FMLP by FNLPNTL-FL after FMLP was bound for 98 s (▲) or 1.5 h (●) before the addition of FNLPNTL-FL. Data were collected using protocol D with the addition of 3 nM FNLPNTL-FL to cells at 10^6/mL at time zero after pre-incubating cells at 10^6/mL with 100 nM FMLP. Data were fit as described in Materials and Methods and reveal two different rates of FNLPNTL-FL binding, indicating a shift toward a higher affinity receptor−FMLP complex with an increase in the time of incubation with FMLP. Data were corrected for nonspecific binding and fit as described in Materials and Methods.

and dissociation of unlabeled ligand, obtained by fitting Model II for the simultaneous presence of FNLPNTL-FL and unlabeled ligand to data collected per protocols C and D, are given in Table 2. Typical fits to competitive association data collected as described in protocol C and displacement data collected as described in protocol D are given for FMLP in Figure 6, panels A and B, respectively. Fits to association and displacement data (for displacement of prebound unlabeled ligand at approximately 90 s) gave estimates for association (k_{f_2}) and dissociation (k_{r_2}) rate constants associated with the low affinity receptor (Table 2). Estimates for k_{c_2} using these two protocols yielded a rate constant of zero for FMLP, FNLP, and t-BOC. Two interpretations are consistent with these last data: (1) the reaction does not occur and k_{c_2} is identically zero, or (2) the reaction is insignificant in the time frame of the data collection. Figure 5 shows the plausibility of the second interpretation if the magnitude of k_{c_2} is on the order of 10^{-4} s^{-1}.

Each Ligand Tested Exhibited Two Affinity States and the Rate Constant for the Conversion of Receptor from Low to High Affinity (k_c and k_{c_2}) Is Different for Different Ligands. To determine if there were two affinity states for the ligands FMLP, FNLP, and t-BOC, the displacement protocol (protocol D) was run for two different preincubation times with the unlabeled ligand, approximately 90 s and approximately 2 h. Typical displacement data for prebound FMLP are shown in Figure 6B. If there were no affinity conversion of the receptor, the kinetics of displacement would have been the same for the two incubation times. Data in Figure 6B clearly indicate that FMLP dissociation is slower after longer incubation times.

Table 3: 37 °C Rate Constants for FNLPNTL-FL Calculated by the Arrhenius Dependency of Reaction on Temperature

parameter	4 °C value (this work)[a]	37 °C value (Arrhenius conv.)	37 °C values (measured)
k_f (M^{-1} s^{-1})	1.1×10^7	5.2×10^7	8.4×10^7 [b]
k_r (s^{-1})	7.3×10^{-2}	3.4×10^{-1}	3.7×10^{-1} [b]
k_c (s^{-1})	1.7×10^{-2}	8.0×10^{-2}	6.5×10^{-2} [b]
			7.0×10^{-2} [c]
k_{f_n} (M^{-1} s^{-1})	2.0×10^6	9.4×10^6	8.4×10^7 [b]
k_{r_n} (s^{-1})	6.9×10^{-4}	3.2×10^{-3}	4.6×10^{-3} [b]
			5.0×10^{-3} [d]

[a] Average values from Table 1. [b] Hoffman et al. (1996). [c] Sklar et al. (1987b). [d] Sklar et al. (1989).

To determine the rate constant of conversion, k_{c_2}, for very slowly converting receptors as seen with FMLP-, FNLP-, and t-BOC-bound receptors, the iterative approach described in Materials and Methods was necessary. From these fits, we obtained estimates for the rate constants of the affinity conversion for each ligand (Table 2). Results indicate that k_{c_2} is on the order of 10^{-4} s^{-1} for FMLP, FNLP, and t-BOC, two orders of magnitude smaller than the analogous rate constant determined for FNLPNTL-FL.

Comparison of Receptor States at 37 and 4 °C. At 37 °C two affinity states of the receptor have been seen, a low affinity form that appears to be LR_s and a high affinity form referred to as LR_x that is insensitive to guanine nucleotide and does not participate in signaling. Presumably an LRG complex exists but is so short-lived that it is not detected in typical binding experiments (Neubig & Sklar, 1993). Comparision of receptor states at 37 and 4 °C was made by performing an Arrhenius conversion of rate constants at 4 °C to their predicted 37 °C values and comparing these values with the experimental values at 37 °C (Table 3). Using an activation energy of 8000 cal/mol (Sklar et al., 1984c), Arrhenius conversions of 4 °C data on FNLPNTL-FL binding to 37 °C estimates for k_f, k_r, k_c, and k_{rn} yielded values that were similar in magnitude to rate constants measured at 37 °C (Hoffman et al., 1996; Sklar et al., 1987, 1989). The value for k_{rn} obtained in this manner, however, was an order of magnitude less than the value of k_{rn} measured at 37 °C. This suggests that whereas the low affinity form of the receptor may be the same species at 4 and 37 °C, the high affinity form may differ in nature.

We then questioned whether R_n observed at 4 °C might represent an LRG species. We reasoned that if an LRG species were observed at 4 °C, PT treatment, which uncouples G from R, would convert all the receptors to LR_s, so only one receptor state would be observed. However, extensive PT treatment did not reduce the binding to a single state model. Thus neither of the receptor species observed at 4 °C represented a receptor precoupled to G_i protein. In addition, receptor interconversion at 4 °C was not affected by extensive PT treatment, yielding results consistent with the G_i-protein-independent receptor conversion observed at 37 °C (Sklar et al., 1989; Hoffman et al., 1996). Figure 7 shows dissociation data of 3 nM FNLPNTL-FL from cells treated with 5 μg/mL of PT for 2 h at 37 °C. For data fits to PT-treated cells, k_f was determined from association data (protocol A) and held constant while k_r, k_c, and k_{r_n} were varied. The value for k_{f_n} was constrained as previously described. Estimated values for k_f, k_r, and k_c were no different ($p < 0.05$, $n = 2$ donors) than those obtained with control cells which were incubated for 2 h at 37 °C without PT (Figure 3B).

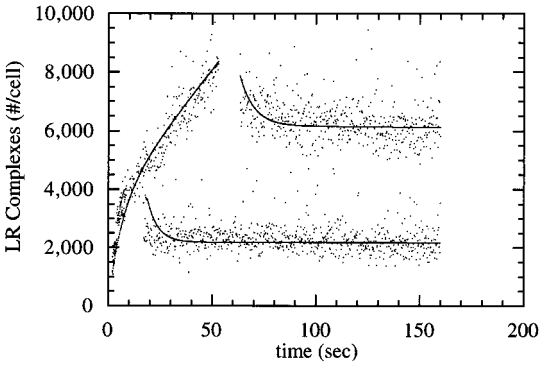

FIGURE 7: Dissociation of 3 nM FNLPNTL-FL from pertussis toxin-treated cells. Cells were incubated with 5 μg/mL pertussis toxin for 2 h at 37 °C. Dissociation data were collected using protocol B, adding 3 nM FNLPNTL-FL to cells at 10^6/mL at time zero, and interrupting binding with 3×10^{-5} M FMLP after 15 and 60 s of ligand binding. Data show the same dissociation characteristics as untreated cells (Figure 3B), indicating a G_i protein-independent conversion of the receptor affinity. Data were corrected for nonspecific binding and fit as described in Materials and Methods.

DISCUSSION

With the aid of high resolution binding data, we determined that there are two affinity states for the N-formyl peptide receptor at 4 °C and that the rate of conversion to a high affinity state is ligand-dependent. Our results supporting two affinity states are different from a large number of investigators who have reported that one-site models adequately describe the affinity of the N-formyl peptide receptor at 4 °C (Goldman et al., 1986; Korchak et al., 1984; Mueller et al., 1991; Sklar et al., 1985a; Tennenberg et al., 1988) but are consistent with the results of Zigmond and Tranquillo (1986) and Vitkauskas et al. (1980), who observed two affinity states in the binding of tritiated FNLP to rabbit neutrophils. There are two plausible reasons that one-site models have given "adequate" fits to most previous data (i.e., no statistical improvement in the fit of data with a two-site model). First, many previous studies simply determined a K_d from equilibrium data. Our data show that such a K_d typically reflects only the high affinity form of the receptor. For FNLPNTL-FL binding, simulations show that the conversion to the high affinity receptor form is complete (99%) in less than 45 min at 4 °C. Second, we suggest that the resolution of kinetic data collected previously [typically one data point every 10 s, e.g., Fay et al. (1991)] was often not sufficient to yield a statistical improvement in the fit with a two-site model. Furthermore, we determined that the fit of the binding model to association data was necessary but not sufficient for determining the adequacy of the binding model, and that dissociation and displacement experiments afford a distinction between one- and two-site models.

The responses of neutrophils to N-formyl peptides are initiated and often saturate well before binding equilibrium has been achieved. Because of this, it is important to understand the kinetics of the ligand−receptor formation in order to test mechanisms that predict response behavior. In this study, we determined the binding kinetics of agonists FNLPNTL-FL, FMLP, and FNLP to both low and high affinity receptors (Tables 1 and 2). To see if differences in the sensitivity of a neutrophil response correlate with K_ds

for the low affinity receptor, we compared dose−response curves for the rate of actin polymerization from Omann and Sklar (1988) with our measured K_d values for the low affinity receptor. Dose−response curves in Omann and Sklar give the rank order potency of agonist: FNLPNTL-FL > FMLP > FNLP with corresponding EC_{50} values of 10^{-11} M, 3×10^{-10} M, and 2×10^{-9} M, respectively. Our work yielded low affinity receptor K_d values consistent with this rank order, giving 6 nM, 49 nM, and 60 nM for FNLPNTL-FL, FMLP, and FNLP, respectively, and identical rank ordering for the high affinity receptor K_d values.

We do not expect K_d values to be sufficient for predicting the relative response of different ligands. Since actin polymerization and oxidant production are initiated within the first several seconds of ligand binding, dynamic information on the duration of a particular ligand−receptor state is important. In this study, we found that the duration of the low affinity N-formyl peptide ligand−receptor complex is not governed solely by the dissociation rate constant of the ligand but also by the conversion rate from low to high affinity receptor. Our results yielded a conversion rate constant on the order of 10^{-2} s^{-1} for FNLPNTL-FL and 10^{-4} s^{-1} for FNLP, FMLP, and the N-formyl peptide receptor antagonist t-BOC. This conversion rate constant for FNLP is consistent with a value of 1.4×10^{-4} s^{-1} estimated by Zigmond and Tranquillo (1986) for tritiated FNLP binding in rabbit neutrophils. Conversion rate constants for the other ligands have not been previously published.

In comparing agonists and antagonist, we note first that for agonists the values of k_f and k_{f_2} were very similar and the values of k_{r_n} and $k_{r_{n2}}$ varied by less than a factor of 10, whereas k_r and k_{r_2}, and also k_c and k_{c_2}, varied over two orders of magnitude. The largest variation was seen in k_{fn} and $k_{f_{n2}}$, which varied from 43 to 2×10^6 M^{-1} s^{-1}. Values for the rate parameters obtained for the antagonist (t-BOC) fell within the ranges of those of the agonists except for k_{f_2}. k_{f_2} for t-BOC was approximately 2 orders of magnitude less than that of the agonists, suggesting that the rate of ligand binding to the low affinity form of the receptor may be important for determining activity.

It is noteworthy that binding of the antagonist caused the interconversion of receptor states, a process that one might think requires some type of cell activation. However, we note that interconversion of receptor states by agonists occurred in pertussis toxin treated cells in which receptors were uncoupled from the G protein mediated signal transduction pathway. Thus it appeared that although antagonists did not bind to receptors in a manner that communicated with G proteins, the antagonist did bind in a manner that activated receptor processing pathways.

In order to relate receptor−ligand complex generation to responses, it is important to determine the extent to which each receptor state, LR_s or LR_n, is capable of signaling. When compared to experimental data from the literature, simulations utilizing conversion rate constants determined in this study yield results that are consistent with the hypothesis that LR_s is a signaling form. Data from Zigmond and colleagues (Zigmond & Tranquillo, 1986) demonstrated that, after 2 h of FNLP binding at 4 °C, a chemotactic response could still be generated. Simulations using rate constants given in Table 2 and our two-state model indicate that roughly one-third of the total receptors remain in the LR_s state after 2 h of FNLP binding at 4 °C, and data that relate LR_s complex formation with responses at 37 °C (Hoffman et al., 1996) suggest that this quantity is more than sufficient for generating an actin polymerization response. Similar actin polymerization response data for cells prebound with FMLP or FNLPNTL-FL at 4 °C for 30 min are given in Model and Omann (1995). They showed that cells prebound with FMLP or FNLPNTL-FL were capable of producing actin polymerization responses after the temperature of the cell suspension was elevated to 16 °C. Simulations using rate constants given in Tables 1 and 2 indicate that for both ligands there are a sufficient number of LR_s complexes present after 30 min of binding at 4 °C to generate a response. However, in preliminary experiments [G. M. Omann and M. L. Keil, unpublished data], we have extended the time-course of the Model and Omann (1995) protocol out to 1 h of prebinding at 4 °C with FNLPNTL-FL, where simulations predicted there were no LR_s and R_s remaining, and the actin polymerization response still occurred. Since the actin assay was performed at 16 °C, it was unlikely that significant upregulation of new R_s could have occurred to accommodate the response. Thus it appears that LR_n is also capable of signaling a response.

Is LR_n the same entity as the high affinity state found at 37 °C (Jesaitis & Klotz, 1993; Jesaitis et al., 1984, 1988a,b, 1989; Klotz et al., 1994; Klotz & Jesaitis, 1994)? In this work we determined that the high affinity state, LR_n, is not a G_i protein-coupled form of the receptor and that the conversion itself is also G_i protein insensitive. The latter result is analogous to the G_i protein insensitive conversion of receptor states observed at 37 °C (Sklar et al., 1989) and suggests that the nature of the conversion to the high affinity state is similar at 4 and 37 °C. However, the high affinity receptor at 37 °C appears to be a nonsignaling form of the receptor, contrary to our preliminary data cited above. The order of magnitude difference in the Arrhenius conversion of the value of k_{f_n} with the value measured at 37 °C (see Table 3) suggests that there may be a difference in the biochemical nature of the ligand binding pocket for the high affinity state at different temperatures. Whether the receptor states themselves are biochemically similar is yet to be elucidated. It is possible that R_n is a receptor state that appears transiently at 37 °C and is not detected in binding studies at 37 °C because it is rapidly converted to LR_x. From analogy with other systems, the desensitized receptor state LR_x could be a phosphorylated receptor or X could be an arrestin-like molecule. N-formyl peptide receptor phosphorylation has been shown to occur (Ali et al., 1993; Tardif et al., 1993); however, whether or not LR_x is a phosphorylated receptor is not known, and arrestin-like molecules have not been identified in neutrophils. Definitive identification of the nature of LR_n and the high affinity form at 37 °C awaits more detailed biochemical (versus functional) studies. Understanding the nature of these receptor forms may afford explanations for observed differences in agonist potency that is unexplained by differences in affinities of the ligand for the receptor and yield insight into the mechanism of the conversion of receptor from the active to inactive form.

ACKNOWLEDGMENT

We thank Anna Waller for help with data analysis.

APPENDIX

Equations A.1−A.9 describe the two-site model (Model II) and are used to fit FNLPNTL-FL binding data and

competitive binding data. When there is no competitive ligand present, the initial value for [A] is equal to zero.

The total (apparent) number of ligand−receptor complexes, $[LR]_{app}$, is given by

$$[LR]_{app} = [LR_s] + [LR_n] \quad (A.1)$$

The two states of the LR complex are given by

$$\frac{d[LR_s]}{dt} = k_f[L][R_s] - (k_r + k_c)[LR_s] \quad (A.2)$$

$$\frac{d[LR_n]}{dt} = k_c[LR_s] + k_{f_n}[L][R_n] - k_{r_n}[LR_n] \quad (A.3)$$

The two states of the AR complex are given by

$$\frac{d[AR_s]}{dt} = k_{f_2}[A][R_s] - (k_{r_2} + k_{c_2})[AR_s] \quad (A.4)$$

$$\frac{d[AR_n]}{dt} = k_{c_2}[AR_s] + k_{f_{n2}}[A][R_n] - k_{r_{n2}}[AR_n] \quad (A.5)$$

Finally, the quantities of free receptor and ligand are given by

$$\frac{d[R_s]}{dt} = k_r[LR_s] - k_f[L][R_s] - k_{f_2}[A][R_s] + k_{r_2}[AR_s] \quad (A.6)$$

$$\frac{d[R_n]}{dt} = k_{r_n}[LR_n] - k_{f_n}[L][R_n] + k_{r_{n2}}[AR_n] - k_{f_{n2}}[A][R_n] \quad (A.7)$$

$$\frac{d[L]}{dt} = [-k_f[L][R_s] + k_r[LR_s] + k_{r_n}[LR_n] - k_{f_n}[L][R_n]][n(Av)^{-1}(V)^{-1}] \quad (A.8)$$

$$\frac{d[A]}{dt} = [-k_{f_2}[A][R_s] + k_{r_2}[AR_s] + k_{r_{n2}}[ARn] - k_{f_{n2}}[A][R_n]][n(Av)^{-1}(V)^{-1}] \quad (A.9)$$

where Av is Avogadro's number, n is the number of cells in the assay volume, and V is the assay volume in liters.

REFERENCES

Ali, H., Richardson, R. M., Tomhave, E. D., Didsbury, J. R., & Snyderman, R. (1993) *J. Biol. Chem. 268*, 24247−24254.

Baggiolini, M., Boulay, F., Badwey, J. A., & Curnutte, J. T. (1993) *FASEB J. 7*, 1004−1010.

Downey, G. P. (1994) *Curr. Opin. Immunol. 6*, 113−124.

Fay, S. P., Posner, R. G., Swann, W. N., & Sklar, L. A. (1991) *Biochemistry 30*, 5066−5075.

Finney, D. A., & Sklar, L. A. (1983) *Cytometry 4*, 54−60.

Goldman, D. W., Enkel, H., Gifford, L. A., Chenoweth, D. E., & Rosenbaum, J. T. (1986) *J. Immunol. 137*, 1971−1976.

Hoffman, J. F., Linderman, J. J., & Omann, G. M. (1996) *J. Biol. Chem. 271*, 18394−18404.

Hyslop, P. A., & Sklar, L. A. (1984) *Anal. Biochem. 141*, 280−286.

Jacobs, A. A., Huber, J. L., Ward, R. A., Klein, J. B., & McLeish, K. R. (1995) *J. Leukocyte Biol. 57*, 679−686.

Jesaitis, A. J., & Klotz, K. N. (1993) *Eur. J. Haematol. 51*, 288−293.

Jesaitis, A. J., Naemura, J. R., Painter, R. G., Sklar, L. A., & Cochrane, C. G. (1983) *J. Biol. Chem. 258*, 1968−1977.

Jesaitis, A. J., Naemura, J. R., Sklar, L. A., Cochrane, C. G., & Painter, R. G. (1984) *J. Cell Biol. 98*, 1378−1387.

Jesaitis, A. J., Bokoch, G. M., Tolley, J. O., & Allen, R. A. (1988a) *J. Cell Biol. 107*, 921−928.

Jesaitis, A. J., Bokoch, G. M., & Allen, R. A. (1988b) *Signal Transduction in Cytoplasmic Organization and Cell Motility* (Condeelis, J., Satir, P., & Lazarides, E., Eds.) pp 325−337, Alan Liss, New York.

Jesaitis, A. J., Tolley, J. O., Bokoch, G. M., & Allen, R. A. (1989) *J. Cell Biol. 109*, 2783−2790.

Kenakin, T. (1993) in *Pharmacologic Analysis of Drug-Receptor Interaction*, Raven Press, Ltd., New York.

Klotz, K.-N., & Jesaitis, A. J. (1994) *BioEssays 16*, 193−198.

Klotz, K.-N., Krotec, K. L., Gripentrog, J., & Jesaitis, A. J. (1994) *J. Immunol. 152*, 801−810.

Koo, C., Lefkowitz, R. J., & Snyderman, R. (1982) *Biochem. Biophys. Res. Commun. 106*, 442−449.

Korchak, H. M., Wilkenfeld, C., Rich, A. M., Radin, A. R., Vienne, K., & Rutherford, L. E. (1984) *J. Biol. Chem. 259*, 7439−7445.

Lad, P. M., Kaptein, J. S., Lin, C. K., Kalunta, C. I., Scott, S. J., & Gu, D. G. (1992*) Immunol. Ser. 57*, 107−136.

Low, D. A., Baker, J. B., Koonce, W. C., & Cunningham, D. D. (1981) *Proc. Natl. Acad. Sci. U.S.A. 78*, 2340−2344.

Mueller, H., Weingarten, R., Ransnas, L. A., Bokoch, G. M., & Sklar, L. A. (1991) *J. Biol. Chem. 266*, 12939−12943.

Model, M. A., & Omann, G. M. (1995) *J. Leukocyte Biol. 58*, 1−11.

Mood, A. M., Graybill, F. A., & Boes, D. C. (1974) in *Introduction to the Theory of Statistics*, McGraw-Hill, Inc., New York.

Neubig, R. R., & Sklar, L. A. (1993) *Mol. Pharmacol. 43*, 734−740.

Norgauer, J., Eberle, M., Fay, S. P., Lemke, H. D., & Sklar, L. A. (1991) *J. Immunol. 146*, 975−980.

Omann, G. M., & Sklar, L. A. (1988) *J. Cell Biol. 107*, 951−958.

Omann, G. M., Allen, R. A., Bokoch, G. M., Painter, R. G., Traynor, A. E., & Sklar, L. A. (1987) *Physiol. Rev. 67*, 285−322.

Omann, G. M., Harter, J. M., Hasslan, N., Mansfield, P. J., Succhard, S. J., & Neubig, R. R. (1992) *J. Immunol. 149*, 2172−2178.

Painter, R. G., Zahler-Bentz, K., & Dukes, K. (1987) *J. Cell. Biol. 105*, 2959−2971.

Posner, R. G., Fay, S. P., Domalewski, M. D., & Sklar, L. A. (1994) *Mol. Pharmacol. 45*, 65−73.

Seber, G. A. F., & Wild, C. J. (1989) in *Nonlinear Regression*, John Wiley and Sons Inc., New York.

Schonbrunn, A., & Tashjian, A. H., Jr. (1978) *J. Biol. Chem. 253*, 6473−6483.

Sklar, L. A. (1986) *Adv. Immunol. 39*, 95−143.

Sklar, L. A. (1987) *Annu. Rev. Biophys. Biophys. Chem. 16*, 479−506.

Sklar, L. A., & Finney, D. A. (1982) *Cytometry 3*, 161−165.

Sklar, L. A., Jesaitis, J., & Painter, R. G. (1984a) *Contemp. Top. Immunobiol. 14*, 29−81.

Sklar, L. A., Finney, D. A., Oades, Z. G., Jesaitis, J., Painter, R. G., & Cochrane, C. G. (1984b) *J. Biol. Chem. 259*, 5661−5669.

Sklar, L. A., Sayre, J., McNeil, V. M., & Finney, D. A. (1985a) *Mol. Pharmacol. 28*, 323−330.

Sklar, L. A., Hyslop, P. A., Oades, Z. G., Omann, G. M., Jesaitis, J., Painter, R. G., & Cochrane, C. G. (1985b) *J. Biol. Chem. 260*, 11461−11467.

Sklar, L. A., Omann, G. M., & Painter, R. G. (1985c) *J. Cell Biol. 101*, 1161−1166.

Sklar, L. A., Bokoch, G. M., Button, D., & Smolen, J. E. (1987) *J. Biol. Chem. 262*, 135−139.

Sklar, L. A., Mueller, H., Omann, G., & Oades, Z. (1989) *J. Biol. Chem. 264*, 8483−8486.

Tardif, M., Mery, L., Brouchon, L., & Boulay, F. (1993) *J. Immunol. 150*, 3534−3545.

Tennenberg, S. D., Zemlan, F. P., & Solomkin, J. S. (1988) *J. Immunol. 141*, 3937−3944.

Tolley, J. O., Omann, G. M., & Jesaitis, A. J. (1987) *J. Leukocyte Biol. 42*, 43−50.

Vitkauskas, G., Showell, H. J., & Becker, E. L. (1980) *Mol. Immunol. 17*, 171−180.

Zigmond, S. H., & Tranquillo, A. W. (1986) *J. Biol. Chem. 261*, 5283−5288.

BI961088P